J Polym Res (2015) 22: 181
DOI 10.1007/s10965-015-0822-3

ORIGINAL PAPER

Optimized synthesis and swelling properties of a pH-sensitive semi-IPN superabsorbent polymer based on sodium alginate-*g*-poly(acrylic acid-*co*-acrylamide) and polyvinylpyrrolidone and obtained via microwave irradiation

Mohammad Tally[1] · **Yomen Atassi**[1]

Received: 26 January 2015 / Accepted: 3 August 2015 / Published online: 22 August 2015

Abstract A pH-sensitive superabsorbent hydrogel composite, sodium alginate-*g*-poly(acrylic acid-co-acrylamide) in the presence of polyvinylpyrrolidone (PVP), was prepared using the semi-interpenetrating polymer network (semi-IPN) technique and microwave irradiation. Potassium peroxodisulfate (KPS) was used as an initiator, *N*,*N*,*N*′,*N*′-tetramethylene diamine (TEMED) as a reaction accelerator, and *N*,*N*′-methylene bisacrylamide (MBA) as a crosslinker. The Taguchi method was employed to optimize the synthetic conditions for the hydrogel based on water absorbency. The Taguchi L_9 (3^4) orthogonal array was selected for the experimental design. The mass concentrations of MBA (C_{MBA}), KPS (C_{KPS}), and sodium alginate (C_{NaAlg}) as well as the molar ratio of acrylamide to acrylic acid ($R_{AM/AA}$) were chosen as the four factors in the design. Based on an analysis of variance in the test results, the optimal conditions were found to be 0.18 g/L of MBA, 0.60 g/L of KPS, 7.73 g/L of NaAlg, and $R_{AM/AA}$ = 1:1. The maximum water absorbency of the optimized hydrogel was found to be 1551 g/g. The relative thermal stability of the hydrogel in comparison with sodium alginate was proven using thermogravimetric analysis. The prepared hydrogel was characterized by FTIR and scanning electron microscopy (SEM). The influences of environmental parameters such as the pH and the ionic strength of the solution on the water absorbency were also investigated.

✉ Yomen Atassi
yomen.atassi@hiast.edu.sy

[1] Laboratory of Materials Science, Department of Applied Physics, Higher Institute for Applied Science and Technology, P.O. Box 31983, Damascus, Syria

Keywords Sodium alginate · Superabsorbent polymers · Polyacrylate · Polyacrylamide · Semi-interpenetrating polymer network · Microwave synthesis

Introduction

Superabsorbent polymers (SAPs) are materials that can absorb large amounts of water and even retain this absorbed water when pressure (below a certain value) is applied [1]. SAPs are widely used in many fields, such as hygiene products, agriculture, and soil conditioning [2]. They can also be used in controlled drug-delivery systems, artificial snow, swelling rubber, and in waste treatments where water absorbency or water retention is important [3]. Most of these polymers are prepared from nonrenewable chemical raw materials and the monomers are relatively expensive. Fortunately, there is increasing interest in using renewable natural resources to generate these polymers. Substances such as starch [4], chitosan [5], cellulose [6], carrageenan [7], pectin [8], protein [9], collagen [10], sugarcane bagasse [11], and lignin (and/or lignosulfonate) [12] are currently employed in the preparation of SAPs.

Sodium alginate (NaAlg) is an anionic polysaccharide composed of varying proportions of poly-β-1,4-D-mannuronic acid ("M units") and α-1,4-L-glucuronic acid ("G units") connected by 1–4 linkages. NaAlg can be extracted from brown algae, so it is abundant, renewable, nontoxic, water-soluble, biodegradable, and biocompatible [13]. In addition, NaAlg can easily be modified through various chemical or physical methods such as grafting copolymerization with hydrophilic vinyl monomers [14], by blending polymers [15], and by compounding with other functional components [16]. Due to these advantages and because of its ability to gelatinize, NaAlg has received considerable attention in industrial and medical fields [17]. The grafting technique is a

useful tool for obtaining polymers with new properties. The graft copolymerization of vinyl monomers with alginate can introduce desirable properties and enlarge the field of potential applications of alginate through the appropriate selection of side chains such as polymethyl acrylate [18], polyacrylamide [19], polyacrylonitrile [20], and polyitaconic acid [14].

Conventional thermal heating methods usually take a long time and consume a great deal of energy. On the other hand, microwave irradiation is a promising heating technique due to its specificity in terms of reactivity and its ability to rapidly heat bulk masses [21, 22]. Microwave irradiation has been used for various polymerization reactions such as polycondensation, controlled free-radical polymerization, and ring-opening polymerization [23]. The graft copolymerization of vinyl monomers onto natural polymers has been successfully conducted under microwave irradiation, including the grafting of acrylonitrile onto guar gum [24], the grafting of acrylamide onto chitosan [25], the grafting of acrylic acid onto *Artemisia* seed gum [26], and the grafting of methyl methacrylate onto bamboo cellulose [27]. Recently, a few works have studied the grafting of vinyl monomers onto sodium alginate using microwave irradiation [28–30].

Semi-interpenetrating polymer network (semi-IPN) preparation is a technique involving the blending of two polymers where only one of them is crosslinked in the presence of the other one. It is considered an easy-to-perform technology that can be used to design multicomponent materials [13, 31].

Polyvinylpyrrolidone (PVP) is a nonionic and water-soluble linear polymer. It has been successfully used in pharmaceuticals, cosmetics, foods, printing inks, textiles, and many other fields due to its good solubility, high affinity for various polymers and resins, nontoxicity, biodegradability, and compatibility. PVP is considered a promising candidate to use in the preparation of semi-IPN hydrogels because of its compatibility. The preparation of a new type of superabsorbent polymer with an improved structure and enhanced performance by effectively combining PVP with NaAlg grafted onto a conventional hydrogel has been proposed [13, 22].

The Taguchi method is a powerful experimental design tool developed by G. Taguchi [32]. It can provide a simple, efficient, and systematic approach to optimizing designs in terms of performance, quality, and cost [12]. Many studies have used this method to optimize the conditions used in syntheses [33, 34].

In the study reported in the present paper, sodium alginate (NaAlg) was graft-copolymerized with partially neutralized acrylic acid (AA) and acrylamide (AM) in the presence of polyvinylpyrrolidone (PVP) to produce a new kind of SAP: NaAlg-*g*-P(AA-*co*-AM)/PVP. The Taguchi orthogonal experimental design method was applied to optimize the conditions applied in this synthesis. Introducing sodium alginate into an acrylic SAP not only improves the cost-effectiveness of preparing a SAP; it also improves the properties of that SAP. The resulting optimized NaAlg-*g*-P(AA-*co*-AM)/PVP hydrogel shows good water absorbency (1551 g/g). Morphological and structural characterization of the prepared SAP was implemented using scanning electron microscopy and FTIR spectroscopy.

Experimental

Materials

Sodium alginate (NaAlg, viscosity of the aqueous solution at a concentration of 1 % was 5.0–40.0 cps at 25 °C) and polyvinylpyrrolidone (PVP, MW = 10,000 g/mol) were purchased from Sigma–Aldrich (St. Louis, MO, USA). Acrylic acid (AA) and acrylamide (AM) for synthesis were from Merck (Darmstadt, Germany) and were used as purchased. Potassium peroxodisulfate ($K_2S_2O_8$; KPS) GR for analysis, used as an initiator; *N*,*N*′-methylene bisacrylamide (MBA; special grade for molecular biology), used in electrophoresis as a crosslinker; and *N*,*N*,*N*′,*N*′-tetramethylene diamine (TEMED) GR for analysis, used as an accelerator, were also obtained from Merck. Sodium hydroxide (NaOH, microgranular pure; POCH, Gliwice, Poland) was used for acid neutralization.

The solvents methanol and ethanol (GR for analysis) were obtained from Merck. Saline solutions of sodium chloride (NaCl), magnesium chloride ($MgCl_2$), and aluminum chloride ($AlCl_3$) were prepared with distilled water and were all purchased from Merck (GR for analysis).

Instrumental analysis

IR spectra in the 400–4000 cm^{-1} range were recorded at room temperature on an infrared spectrophotometer (Vector 22, Bruker, Ettlingen, Germany). Before recording IR spectra, powders were mixed with KBr in the ratio 1:250 by weight to ensure uniform dispersion in the KBr pellet. The mixed powders were then pressed in a cylindrical die to obtain clean discs approximately 1 mm thick.

Thermogravimetric analyses of sodium alginate (NaAlg) and the superabsorbent hydrogel were performed (TG-DSC 1600 °C, Labsys, SETARAM, Caluire, France) from room temperature to 600 °C at a heating rate of 10 °C/min and under an argon atmosphere.

The morphology of each sample was examined using a scanning electron microscope (VEGA II SEM instrument, TESCAN, Brno, Czech Republic) after coating the samples with graphite.

Swelling measurements

The water absorbency of the hydrogel was measured by the free swelling method and was calculated in grams of water per

gram of the hydrogel. Thus, an accurately weighed quantity of the polymer under investigation (0.1 g) was immersed in 500 mL of distilled water at room temperature for at least 4 h. Then the swollen sample waas filtered through a weighed 100-mesh (150 μm) sieve until water ceased to drop.

The weight of the hydrogel containing absorbed water was measured after draining for 1 h, and the water absorbency was calculated according to the following equation:

$$S_{eq} = (w_s - w_d)/w_d,$$

where S_{eq} is the equilibrium water absorption calculated in grams of water per gram of superabsorbent sample; w_d and w_s are the weights of the dry sample and the swollen sample, respectively [35, 36].

Swelling kinetics at different pH values

To investigate the rate of absorbency of each SAP at different pH values, accurately weighed quantities (0.1 g) of the polymer under investigation were immersed at room temperature in 500-mL aqueous solutions at different pH values (4.0, 7.0, and 12.0). At consecutive time intervals, the water absorbency of each SAP was measured according to the abovementioned method.

Gel content

In order to measure the gel content, accurately weighed dried samples of the SAP with and without PVP (i.e., NaAlg-*g*-P(AA-*co*-AM)/PVP and NaAlg-*g*-P(AA-*co*-AM), respectively) were dispersed in distilled water to fully swell them. The swollen SAPs were then filtered and washed with distilled water frequently. The samples were dewatered in excess ethanol for 48 h and dried at 50 °C for 12 h until the weight of each SAP remained constant. The gel content is defined as [37]

$$\text{Gel}\,(\%) = \frac{W_d}{W_i} \times 100,$$

where W_d is the weight of the dried SAP after extraction and W_i is the initial weight of the SAP.

Experimental design

The Taguchi orthogonal experimental design technique was used to minimize the number of experiments required and to optimize the synthetic conditions for NaAlg-*g*-P(AA-*co*-AM)/PVP. The distilled water absorbency (S_w) of NaAlg-*g*-P(AA-*co*-AM)/PVP was selected as the response. The following factors were found to be the most influential in the synthesis of NaAlg-*g*-P(AA-*co*-AM)/PVP based on our preliminary experiments and the literature [13]: the mass concentrations of sodium alginate (C_{NaAlg}), the crosslinker MBA (C_{MBA}), and the initiator KPS (C_{KPS}), as well as the molar ratio of AM to AA ($R_{AM/AA}$).

The mass ratio of NaAlg to PVP was kept constant at 1/1.25 since this provided the best dispersion of sodium alginate based on our preliminary trials and according to [13]. The molar ratio of the redox couple KPS/TEMED was also fixed at 1:1 [38]. Thus, we focused on C_{NaAlg} and C_{KPS} as the factors and the corresponding amounts of PVP and TEMED were calculated based on the above remarks.

Our preliminary laboratory trials of the SAPs indicated that three levels should be defined for each selected factor (see Table 1). Thus, the Taguchi L_9 (3^4) orthogonal array was selected for the experimental design. Based on the L_9 orthogonal array, nine syntheses were conducted. Three replicates of each synthesis were performed, so the response for each synthesis was the mean value of the responses obtained in the three replicates. Table 2 shows the experimental design and the corresponding responses S_w.

Preparation of NaAlg-*g*-P(AA-*co*-AM)/PVP semi-IPN SAP

The general procedure employed for the preparation of the superabsorbent polymer through the graft copolymerization of poly(AA-*co*-AM) onto NaAlg in the presence of PVP is now described.

The monomer solutions were prepared as follows. For each run, the total amount of monomers AA and AM was 0.2 mol, and the respective amounts (in mol) of AA and AM were calculated according to the $R_{AM/AA}$ values in Table 1. AA was partially neutralized to 75 wt% by adding NaOH solution (5 M) to the acid in an ice bath to avoid polymerization, and this solution was added to the solution of acrylamide (prepared in ca. 12 mL of distilled water) with continuous stirring. We then added the MBA solution (prepared in ca. 5 mL of distilled water).

According to Table 1, the calculated amounts of NaAlg and PVP needed to give a mass ratio of m(NaAlg)/m(PVP)=0.8 were dissolved in 40 mL of purified water under mechanical stirring to form a relatively sticky solution. This solution was heated to 60 °C using a water bath for 10 min. Two equimolar aqueous solutions of the redox initiator system of KPS and TEMED (each in ca. 5 mL of distilled water) were then

Table 1 Various levels of each factor

Factor	Level 1	Level 2	Level 3
C_{NaAlg} (g/L): A	7.73	10.32	15.48
$R_{AM/AA}$: B	2:1	1:1	1:2
C_{MBA} (g/L): C	0.18	0.36	0.54
C_{KPS} (g/L): D	0.60	1.20	1.50

Table 2 Experimental design (according to $L_9(3^4)$) and the responses

Run	A	B	C	D	S_w (g/g)
1	1	1	1	1	1479
2	1	2	2	2	949
3	1	3	3	3	806
4	2	1	2	3	424
5	2	2	3	1	526
6	2	3	1	2	454
7	3	1	3	2	432
8	3	2	1	3	1114
9	3	3	2	1	738
$\overline{S_W}$	($\overline{S_W}$ is the mean of the S_W values obtained in the nine runs)				769

prepared and added dropwise to the solution of NaAlg under vigorous mechanical stirring. This solution was maintained at 60 °C for 10 min to generate radicals. After cooling this solution to 50 °C, the monomer solution was added dropwise to it under continuous stirring at 1050 rpm for 15 min. The total volume of the reactive mixture was brought up to 100 mL by adding distilled water. The final mixture was then treated in a microwave oven at a power of 950 W. The temperature and viscosity of the mixture increased rapidly. The gelation point was reached after 60 s.

The product (an elastic yellow gel) was cut into small pieces before being washed several times with methanol to dissolve unreacted reagents, washed with ethanol, and dried for several hours at 60 °C until it became solid and brittle. At this point, the solid was ground and treated in the furnace at 60 °C for 24 h.

To prepare the hydrogel without PVP, we used the same procedure as described above but without the addition of PVP.

Results and discussion

Synthesis and mechanistic aspects

The hydrogels were prepared by free-radical polymerization in distilled water under atmospheric conditions. Graft polymerization of acrylamide (AAm) and acrylic acid (AA) onto sodium alginate was carried out in the presence of MBA as a crosslinking agent, potassium persulfate (KPS) as an initiator, and TEMED as a reaction accelerator (Fig. 1). It is supposed that the persulfate decomposes on heating and produces sulfate anion radicals that abstract hydrogen atoms from the hydroxyl groups of sodium alginate to form macroradicals. The active centers radically initiate the polymerization of vinyl monomers, leading to the generation of a graft copolymer. Since a crosslinking agent (MBA) is present, the copolymer possesses a crosslinked structure. The semi-IPN SAP is formed in aqueous solution by synchronous chemical and physical processes that occur between the PVP and the network formed. The linear PVP chains interpenetrate the network and bind to it through hydrogen-bonding interactions.

The polymerization mechanism induced by microwave irradiation is no different from that induced by conventional heating, but the rates of the various reactions that occur during polymerization are higher with microwave irradiation, meaning that the polymerization is achieved rapidly. The time needed for polymerization and gel formation under microwave irradiation is 60 s, while this process takes 3 h under conventional heating at 70 °C [13].

FTIR spectra

Figure 2 shows the FTIR spectra of NaAlg, PVP, the copolymer P(AA-*co*-AM), NaAlg-*g*-P(AA-*co*-AM), NaAlg-*g*-P(AA-*co*-AM)/PVP, and the physical mixture of NaAlg and the copolymer.

In the spectrum for the copolymer hydrogel, the peaks observed at 3430 cm^{-1} and 3208 cm^{-1} correspond to O–H and N–H stretching, respectively. The absorbance at 2948 cm^{-1} is assigned to –C–H stretching of the acrylate group. The peaks at 1674 cm^{-1} and 1565 cm^{-1} are assigned to C=O stretching of the acrylamide groups and acrylate groups, respectively [2, 21].

The characteristic absorption bands of NaAlg at 1103 cm^{-1} and 1030 cm^{-1} (stretching vibrations of C–OH groups) were clearly weaker after the reaction, but these bands were observable in the spectrum for the physical mixture of NaAlg and the copolymer P(AA-*co*-AM) [13].

The absorption bands in the spectrum of NaAlg at 1616 cm^{-1} and 1418 cm^{-1} (from $–COO^-$) shift to 1563 cm^{-1} and 1454 cm^{-1}, respectively, in the spectrum of NaAlg-*g*-P(AA-*co*-AM). The absorption bands at 948 cm^{-1} and 889 cm^{-1} in the spectrum of NaAlg disappear in the spectrum of NaAlg-*g*-P(AA-*co*-AM), while bands at 1170 cm^{-1} and 1674 cm^{-1} appear, which are assigned to the $–COO^-$ stretching of acrylate groups and the C=O stretching of acrylamide groups, respectively. The presence of these bands suggests that grafting of the copolymer onto the sodium alginate backbone has indeed occurred [16].

The characteristic absorption bands of NaAlg at 1616 cm^{-1} (asymmetrical stretching vibrations of $–COO^-$ groups) and 1418 cm^{-1} (symmetrical stretching vibrations of $–COO^-$ groups) overlap with the $–COO^-$ absorption bands of the copolymer in this range [13].

The C=O absorption band of PVP at 1654 cm^{-1} and the –COOH absorption band of NaAlg-*g*-P(AA-*co*-AM) at 1704 cm^{-1} shift to 1671 cm^{-1} after gel formation, suggesting strong hydrogen-bonding interactions between –COOH and –C=O groups [13].

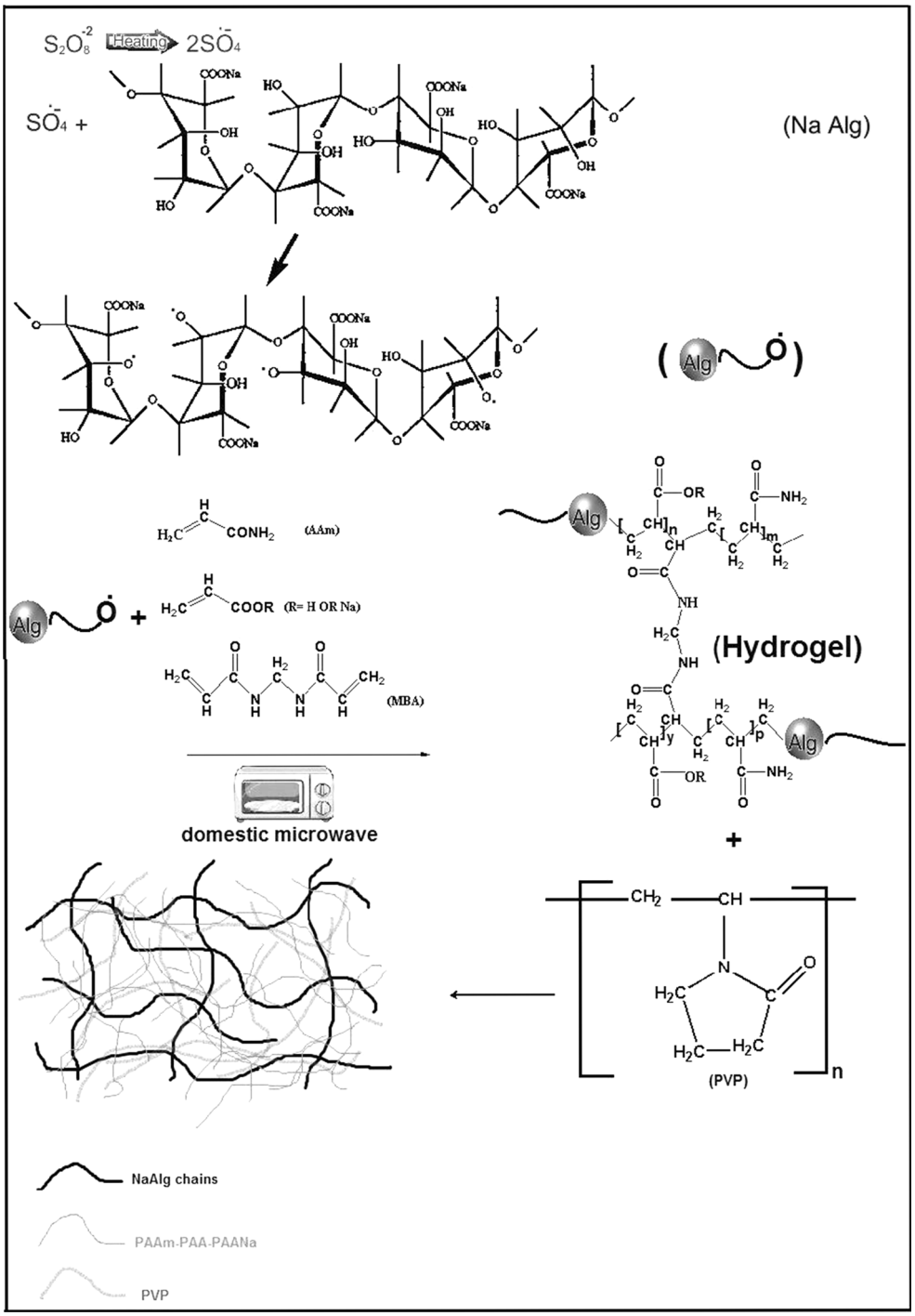

Fig. 1 Proposed mechanistic pathway for the synthesis of NaAlg-*g*-P(AA-*co*-AM)/PVP hydrogel

The characteristic absorption bands of PVP at 1494 cm^{-1}, 1464 cm^{-1}, 1423 cm^{-1} (C–N), and 1288 cm^{-1} also appear in the spectrum of NaAlg-*g*-P(AA-*co*-AM)/PVP at 1491 cm^{-1}, 1458 cm^{-1}, 1419 cm^{-1}, and 1293 cm^{-1}, respectively. This indicates that linear PVP polymer chains are present in the semi-IPN and are linked to the NaAlg-*g*-P(AA-*co*-AM) network by hydrogen-bonding interactions [13].

Morphological analyses

In order to study the change in the surface morphology of the SAP caused by the incorporation of PVP, SEM micrographs of the NaAlg-*g*-P(AA-*co*-AM) and NaAlg-*g*-P(AA-*co*-AM)/PVP semi-IPN SAPs were obtained, as shown in Fig. 3.

NaAlg-*g*-P(AA-*co*-AM) clearly has a smooth and dense surface whereas the NaAlg-*g*-P(AA-*co*-AM)/PVP

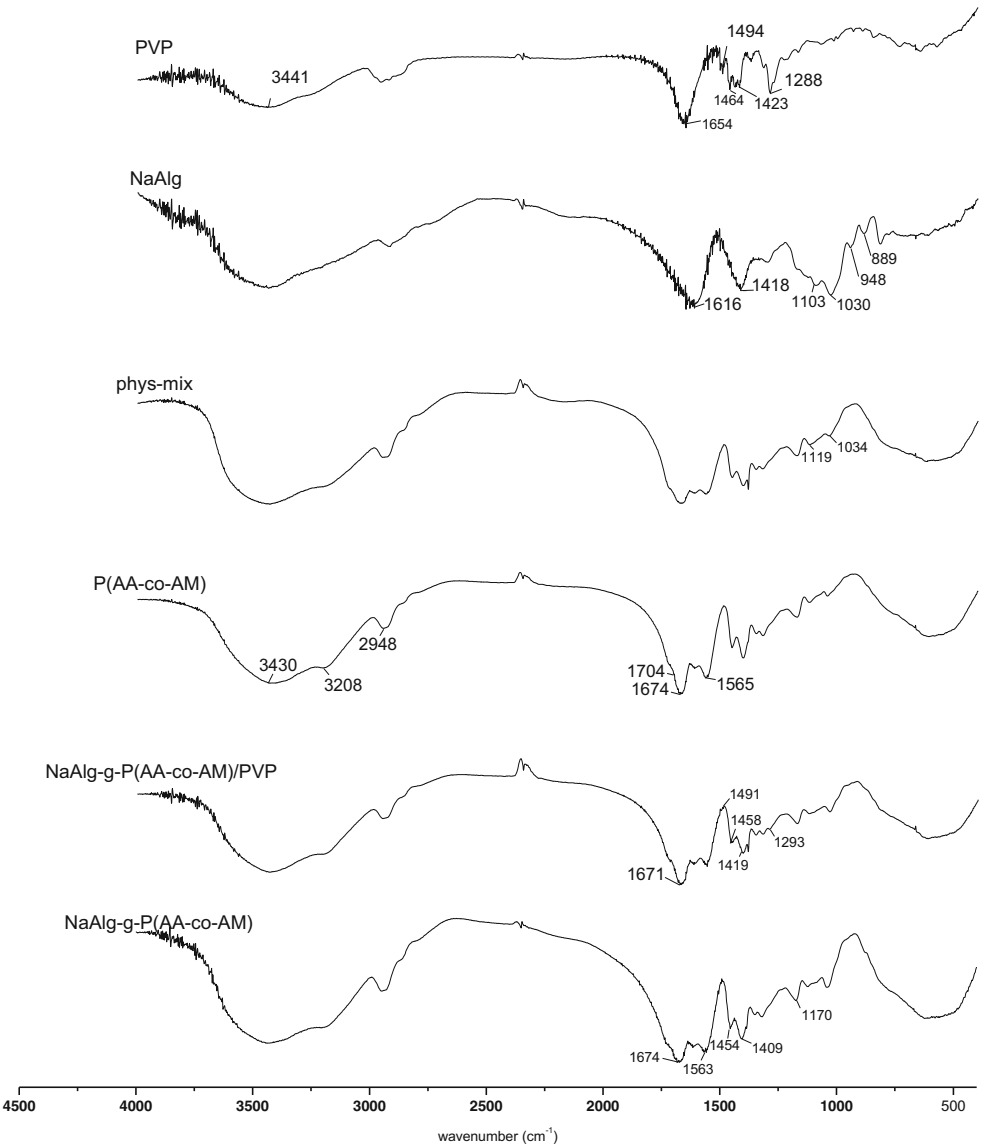

Fig. 2 FTIR spectra of NaAlg, PVP, the copolymer P(AA-*co*-AM), NaAlg-*g*-P(AA-*co*-AM), NaAlg-*g*-P(AA-*co*-AM)/PVP, and the physical mixture of NaAlg and the copolymer

semi-IPN SAP has a comparatively coarse surface. More pores and gaps can be observed on the surface of the NaAlg-*g*-P(AA-*co*-AM)/PVP semi-IPN SAP. This porous structure clearly facilitates the penetration of water and enhances water absorption. These observations indicate that the introduction of PVP improves the surface of the network structure in the SAP. On the other hand, SEM micrographs revealed that PVP effectively interpenetrates the NaAlg-*g*-P(AA-*co*-AM) matrix, with no phase separation observed.

Thermogravimetric analysis

Thermogravimetric degradation curves of the NaAlg and NaAlg-*g*-P(AA-*co*-AM)/PVP semi-IPN in an argon atmosphere are displayed in Fig. 4. The thermogram for NaAlg exhibits two-step degradation behavior: the first step occurs in the temperature range 20–180 °C and can be ascribed to the elimination of free water adsorbed onto the hydrophilic polymer; the other step occurs in the temperature range 200–300 °C and can be assigned to a complex process including dehydration of the saccharide rings and depolymerization with the formation of water, CO_2, and CH_4, as reported in the literature [29]. The temperature that corresponds to 50 % weight loss is 263.85 °C. The thermogram for the NaAlg-*g*-P(AA-*co*-AM)/PVP semi-IPN composite also exhibits two-step degradation behavior. The temperature corresponding to 50 % weight loss is 436.56 °C. From the TG curves, it can be concluded that grafting P(AA-*co*-AM) chains onto the polysaccharide backbone enhances the thermal stability of the polysaccharide, which indicates that the novel SAP was successfully synthesized.

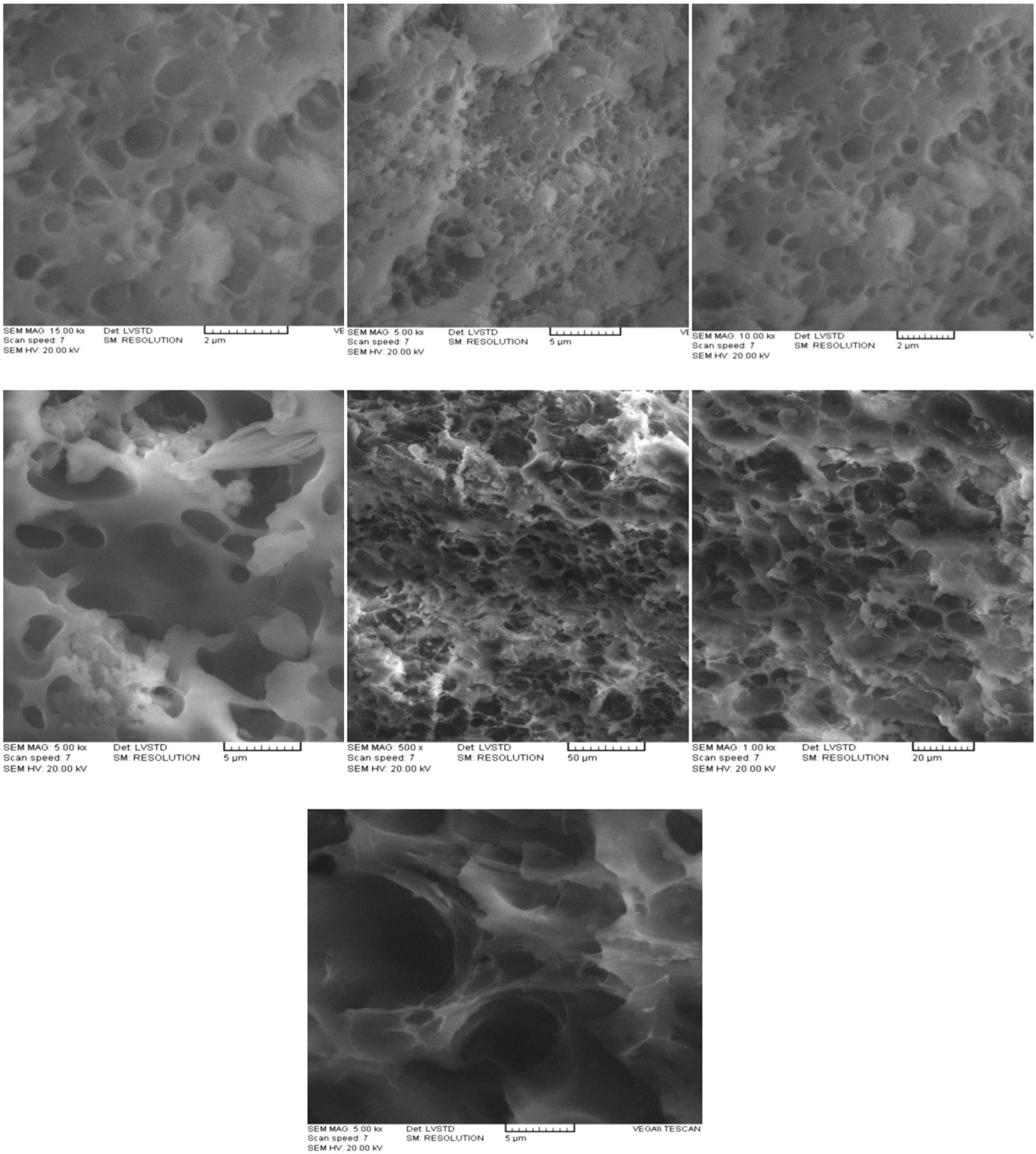

Fig. 3 SEM micrographs of the NaAlg-*g*-P(AA-*co*-AM) SAP (*the first three photos*) and NaAlg-*g*-P(AA-*co*-AM)/PVP semi-IPN composite SAP (*the last four photos*)

Statistical analysis of S_w

The mean value from the three replicates of each S_w response was considered to be the result for each run, and the responses for the nine runs are listed in Table 2. All statistical analysis was conducted using Minitab software (version 16). The signal to noise ratio (S/N ratio) is a very useful parameter for probing the relative effects of factors since it takes both the mean and the variance into consideration and its utilization is strongly suggested by the Taguchi experimental design method employed here. A larger S/N ratio indicates a stronger effect of the factor considered.

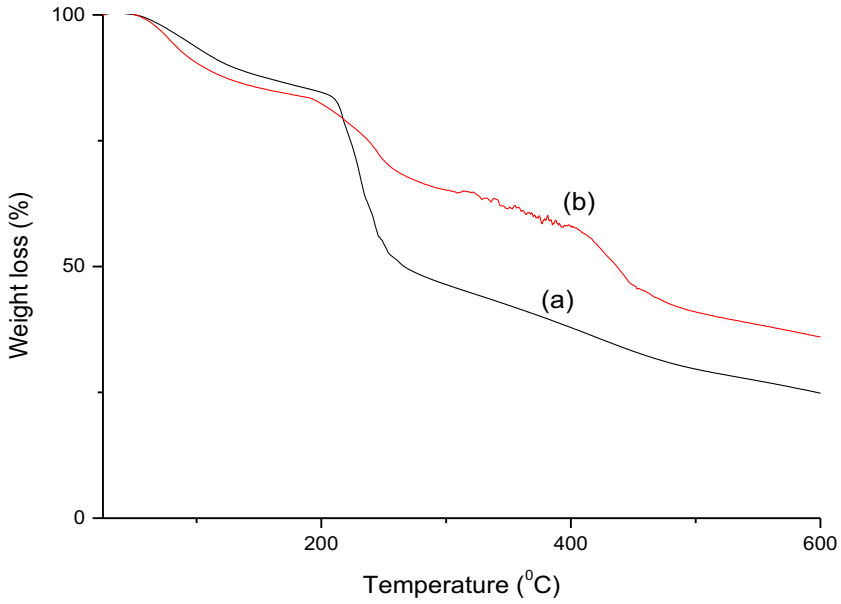

Fig. 4 TGA curves of (*a*) NaAlg and (*b*) NaAlg-*g*-P(AA-*co*-AM)/PVP semi-IPN SAP

The S/N ratio is given by $S/N = -10\log\left[\frac{1}{n}\sum_{i=1}^{n}\frac{1}{y_i^2}\right]$, where y is the response.

Tables 3 and 4 show mean response values and S/N ratios, respectively. The Δ value for each factor is given by Eqs. 1 and 2 (below) for Tables 3 and 4, respectively:

$$\Delta_{\text{factor(mean)}} = \text{response}_{\max} - \text{response}_{\min} \quad (1)$$

$$\Delta_{\text{factor(S/N)}} = S/N_{\max} - S/N_{\min} \quad (2)$$

The order of importance of the factors is the same for Tables 3 and 4: C_{NaAlg}, C_{MBA}, C_{KPS}, $R_{\text{AM/AA}}$.

Figure 5 plots the main effect (reflected in the S/N ratio) for each factor. The optimum level of each factor as indicated by the S/N ratio (based on Table 4 or Fig. 5) is shown in Table 5. The optimal levels of the factors according to the mean responses (i.e., Table 3) are 1 (C_{NaAlg}), 2 ($R_{\text{AM/AA}}$), 1 (C_{MBA}), and 1 (C_{KPS}), which are consistent with those given by the S/N ratio.

Based on the Taguchi method, and taking the contributions of all factors (C_{NaAlg}, $R_{\text{AM/AA}}$, C_{MBA}, C_{KPS}) into account, the value of $S_{\text{w(opt.)}}$ can be predicted as follows:

$$S_{\text{w(opt.)}} = \bar{S_{\text{w}}} + \left[S_{\text{w(NaAlg,1)}} - \bar{S_{\text{w}}}\right] + \left[S_{\text{w(AM/AA,2)}} - \bar{S_{\text{w}}}\right] + \left[S_{\text{w(MBA,1)}} - \bar{S_{\text{w}}}\right] + \left[S_{\text{w(KPS,1)}} - \bar{S_{\text{w}}}\right] =$$
$$S_{\text{w(opt.)}} = 769 + [1078-769] + [1016-769] + [914-769] + [863-769] = 1564 \text{ g/g} \quad ,$$

where $\overline{S_{\text{w}}}$ is the mean value of S_{w} for nine runs shown in Table 2, and $S_{\text{w(NaAlg,1)}}$, $S_{\text{w(AM/AA,2)}}$, $S_{\text{w(MBA,1)}}$, and $S_{\text{w(KPS,1)}}$ are the corresponding mean S_{w} values of the different factors at their optimal levels (Table 5).

Table 3 Response table for mean S_{w} (g/g) values

Level	A, C_{Nalg}	B, $R_{\text{AM/AA}}$	C, C_{MBA}	D, C_{KPS}
1	1078	778	1016	914
2	468	863	704	612
3	761	666	588	781
Δ	610	197	428	302
Rank	1	4	2	3

Table 4 Response table for signal to noise ratios (for S_{w}); larger values are better

Level	A, C_{Nalg}	B, $R_{\text{AM/AA}}$	C, C_{MBA}	D, C_{KPS}
1	60.36	56.22	59.16	58.39
2	53.37	58.30	56.48	55.13
3	57.00	56.21	55.09	57.26
Δ	6.99	2.09	4.07	3.26
Rank	1	4	2	3

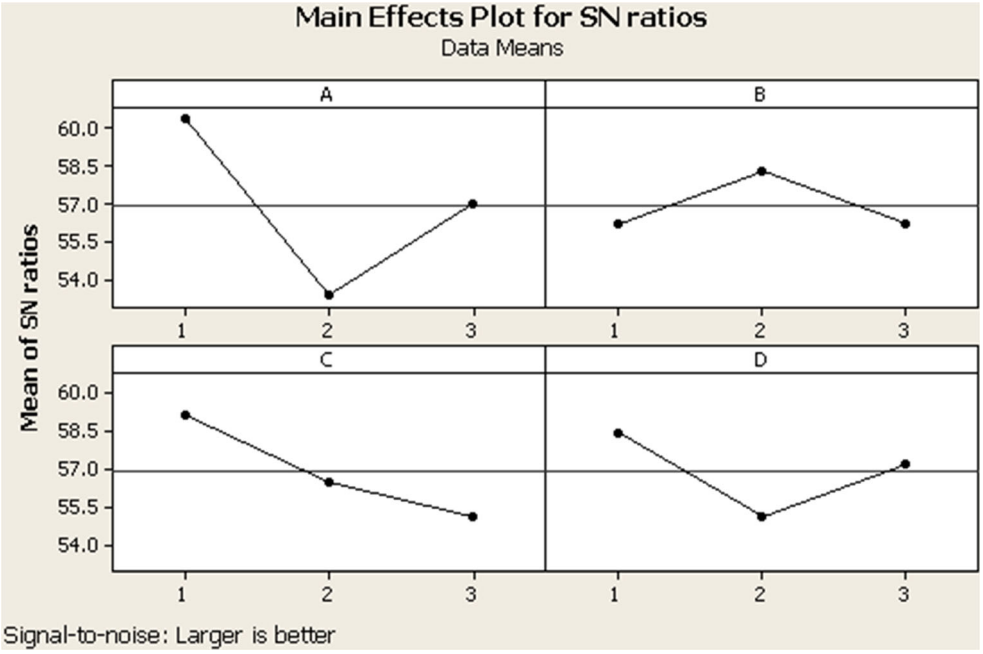

Fig. 5a–d Main effect (reflected in the S/N ratio) of each factor for S_w: **a** C_{Nalg}, **b** $R_{AM/AA}$, **c** C_{MBA}, **d** C_{KPS}

Swelling results

Experiments were conducted to confirm the value of $S_{w(opt.)}$. Three replicates were performed to get the experimental $S_{w(exp.)}$

$$S_{w(exp.)} = 1551 \ \ g/g.$$

The difference between the $S_{w(opt.)}$ value of the optimized SAP and its corresponding experimental value is

$$|S_{w(opt.)} - S_{w(exp.)}| = 1564 - 1551 = 13 \ \ g/g.$$

Therefore, the experimental result is very consistent with the predicted one.

Note that the absorbency of the SAP prepared without PVP is about half of its value when prepared with PVP. This result is in good accord with the SEM results, as the surface of the semi-IPN SAP is more porous. The presence of PVP enhances water absorbency.

The gel contents of the optimized SAP and the SAP without PVP were also measured. They were 55 and 51 %, respectively.

Table 5 Optimum level of each factor for S_w based on Table 4 or Fig. 5

Factor	Rank	Optimum level	Corresponding S_w (g/g)
A	1	1	1078
B	4	2	863
C	2	1	1016
D	3	1	914

Effects of environmental parameters on water absorbency

Effects of the salt solution on water absorbency

The optimized novel SAP was tested to check the effect of the salinity of the swelling solution on its swelling capacity.

Different concentrations of NaCl, $MgCl_2$, and $AlCl_3$ solutions were prepared in order to study the effect of ion charge and ion concentration on water absorption. The absorbency of the synthesized hydrogel was measured using the same procedure adopted when measuring the absorbency with distilled water.

Figure 6 shows that water absorption decreases with increasing ionic strength of the saline solution, as indicated by the Flory equation [39]. The ionic strength of the solution depends on both the concentration and the charge of each individual ion. Also, the presence of ions in the solution decreases the osmotic pressure difference, the driving force for the swelling of the gel with the solution. In addition, multivalent cations (Mg^{2+} and Al^{3+}) can neutralize several charges inside the gel by forming a complex with carboxamide or carboxylate groups, leading to an increased degree of ionic crosslinking and consequently decreased swelling. The effects of the charge on the cation and the cation concentration on the swelling can be concluded from Fig. 6.

Effects of pH on water absorbency and pH-responsive characteristics

Studies have indicated that the water absorption of hydrogels is sensitive to the pH of the environment [40]. Therefore, the swelling behavior of the synthesized SAP was studied at various pH values between 2.0 and 13.0 at room temperature (see

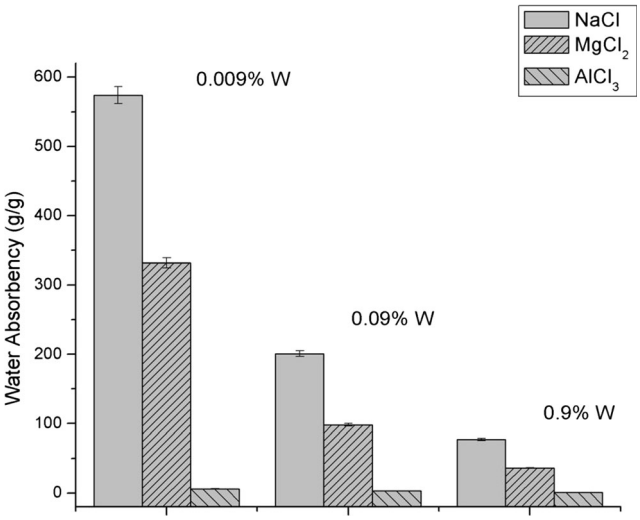

Fig. 6 Histogram showing the water absorbency of the SAP in various saline solutions with different cation charges and cation concentrations

Fig. 7). Since the swelling capacities of all "anionic" hydrogels significantly decrease upon the addition of counter ions (cations) to the swelling medium, and because buffer solutions contain lots of ionic species, no buffer solutions were used as swelling media, as the swelling decreases strongly with increasing ionic strength. Therefore, stock solutions of concentrated HCl and NaOH were diluted with distilled water to reach the desired acidic or basic pH [41].

The absorbency of the synthesized hydrogel was measured using the same procedure adopted in the presence of distilled water.

It is apparent that the SAP barely swells at pH 2, but it swells increasingly as the external pH is raised. We can explain this variation in absorbency with pH as follows. As it is an anionic polymer, the semi-IPN SAP contains numerous hydrophilic groups: $–COO^-$, –COOH, and NH_2. At low pH, sodium carboxylate groups in the polymer network are protonated. Hydrogen-bonding interactions among –COOH and NH_2 groups are strengthened and additional physical crosslinking is generated. However, electrostatic repulsion among $–COO^-$ groups is restricted, so the SAP network tends to shrink and becomes hydrophobic [13]. In the pH interval4–8, some of the carboxylic acid groups are ionized and electrostatic repulsion between the $–COO^-$ groups enhances the swelling capacity [21].

At high pH, the swelling capacity also decreases due to the charge-screening effect of excess Na^+ in the swelling media, which shields the carboxylate anions and prevents effective anion–anion repulsion [21].

These changes in the water absorption of the NaAlg-*g*-P(AA-*co*-AM)/PVP semi-IPN SAP upon altering the pH of the external solution confirm that its swelling behavior is highly pH sensitive.

We also studied the swelling kinetics of the hydrogel at different pH values (see Fig. 8). As can be seen in the figure, the swelling kinetics of the SAP depend on the pH of the swelling medium. The effect of varying the pH on the swelling kinetics was analyzed by applying Schott's pseudo second-order swelling kinetics model [42]:

$$\frac{t}{S_w} = \frac{1}{k_{it}} + \frac{1}{S_\infty} t,$$

where S_w is the swelling ratio at time t, S_∞ is the theoretical equilibrium swelling ratio, and k_{it} is the initial swelling rate constant. According to Fig. 9, plots of average swelling rate (t/

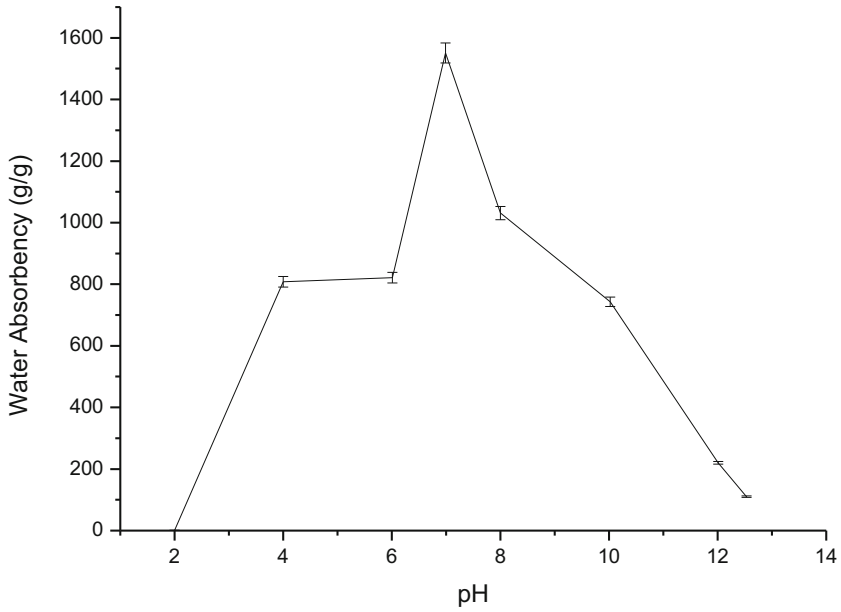

Fig. 7 Effect of environmental pH on water absorbency

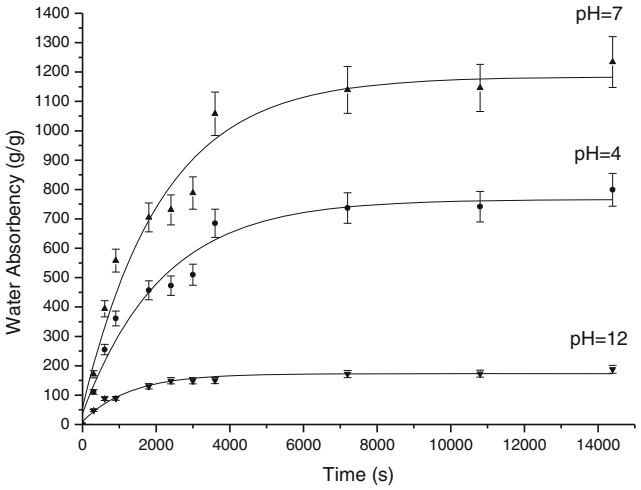

Fig. 8 Swelling kinetics of the hydrogel at different pH values

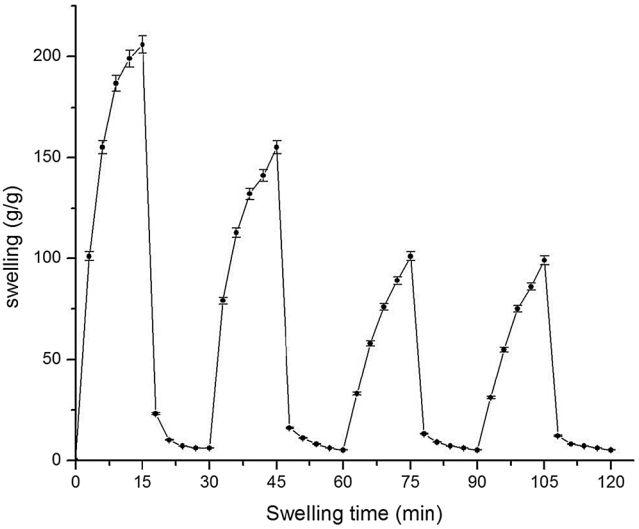

Fig. 10 Swelling–deswelling behavior of the SAP when the pH of the swelling solution was alternated between 7.0 and 2.0. The time interval between pH changes was 15 min

S_w) versus swelling time (t) give straight lines (R^2>0.999), indicating that the swelling process is well fitted by the pseudo second-order swelling kinetic model. The values of k_{it} and S_∞ can be calculated from the slope and intercept of the fitted straight line. The k_{it} values for pH values of4.0, 7.0, and 12.0 are, respectively, 0.520, 0.803, and 0.209 g/(g s). The S_∞ values are 885, 1368, and 195 g/g, respectively. The S_{eq} values (808, 1234, and 188 g/g) are almost equal to the corresponding S_∞ values, which suggests that the SAP reached about 93 % of its equilibrium absorbency within 4 h in the solutions at different pH values. The trend in k_{it} as a function of pH values is similar to that seen for S_∞. The initial swelling rate of the SAP is related to the relaxation rate of the chain segments in the network. Ionization of carboxylate groups occurs at pH>4.7, and increases with increasing pH. Increasing the number of carboxylate groups leads to stronger electrostatic repulsion, which aids the relaxation of the polymer network. This fast relaxation facilitates the penetration of water molecules into the gel network, thus enhancing the initial swelling rate. However, at higher pH values(>10), the mobility of the polymer network is reduced by the screening effect of cations, which limits the diffusion of water molecules into the polymer network and so decreases the initial swelling rate.

Since the swelling behavior of the semi-IPN SAP varies depending on the pH, we investigated the reversibility of the variations in swelling behavior with changes in pH in aqueous solutions at pH values of 2.0 and 7.0. Figure 10 shows the stepwise reproducible changes in the swelling of the SAP at 25 °C that occurred when the pH was alternated between 2.0 and 7.0. The time interval between changes in pH was 15 min. At pH 7.0, the hydrogel swells due to anion–anion repulsive electrostatic forces, while it shrinks within a few minutes at pH 2.0 due to the protonation of carboxylate groups. This rapid swelling–deswelling behavior of the SAP makes it a suitable candidate for controlled-release systems.

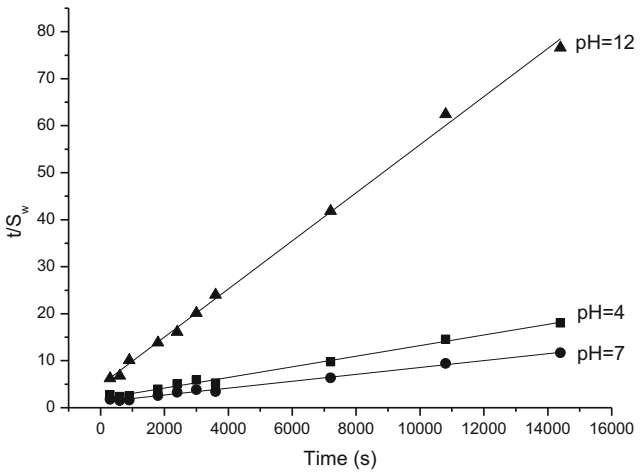

Fig. 9 Schott's pseudo second-order swelling kinetics model

Conclusion

In this work, we successfully prepared a new semi-IPN SAP with an improved structure using a renewable and biodegradable substrate (sodium alginate) and a biocompatible polymer (PVP).

This new type of semi-IPN SAP consisting of NaAlg-*g*-P(AA-*co*-AM) and PVP was synthesized by free-radical graft copolymerization and the semi-interpenetrating technique via microwave irradiation. This preparation method is fast and simple, and it does not require the use of an inert gas during synthesis.

FTIR analysis confirmed that copolymer P(AA-*co*-AM) chains were indeed grafted onto macromolecular chains of NaAlg, and that PVP chains interpenetrated the polymer network and were linked to it via hydrogen-bonding interactions. The surface morphology and swelling capacity of the prepared semi-IPN SAP were greatly improved. This new semi-IPN SAP also exhibited excellent pH sensitivity. It is a promising candidate for use in drug-delivery systems and water-controllable materials.

References

1. Dubrovskii SA, Afanas'eva MV, Lagutina MA, Kazanskii KS (1990) Comprehensive characterization of superabsorbent polymer hydrogels. Polym Bull 24:107–113
2. Spagnol C, Rodrigues FHA, Neto AGVC, Pereira AGB, Fajardo AR, Radovanovic E, Rubira AF, Muniz EC (2012) Nanocomposites based on poly(acrylamide-co-acrylate) and cellulose nanowhiskers. Eur Polym J 48:454–463
3. Liu Y, Cui Y, Yin G, Ma H (2009) Synthesis, characterization, and drug release behavior of novel soy protein/poly(acrylic acid). Iran Polym J 18:339–348
4. Tan Y, Wang P, Xu K, Li W, An H, Li L, Liu C, Dong L (2009) Designing starch-based nanospheres to make hydrogels with high mechanical strength. Macromol Mater Eng 294:855–859
5. Kabiri K, Mirzadeh H, Zohuriaan-Mehr MJ, Daliric M (2009) Chitosan-modified nanoclay-poly(AMPS) nanocomposite hydrogels with improved gel strength. Polym Int 58:1252–1259
6. Sannino A, Mdaghiele M, Demitri C, Scalera F, Esposito A, Esposito V, Maffezzoli A (2010) Development and characterization of cellulose-based hydrogels for use as dietary bulking agents. J Appl Polym Sci 115:1438–1444
7. Pourjavadi A, Amini-Fazl MS, Barzegar S (2008) Optimization of synthesis conditions of a novel carrageenan-based superabsorbent hydrogel by Taguchi method and investigation of its metal ions adsorption. J Appl Polym Sci 107:2970–2976
8. Pourjavadi A, Barzegar S (2009) Smart pectin-based superabsorbent hydrogel as a matrix for ibuprofen as an oral non-steroidal anti-inflammatory drug delivery. Starch/Stärke 61:173–187
9. Lin H, Sritham E, Lim S, Cui Y, Gunasekaran S (2010) Synthesis and characterization of pH- and salt-sensitive hydrogel based on chemically modified poultry feather protein isolate. J Appl Polym Sci 116:602–609
10. Pourjavadi A, Ayyari M, Amini-Fazl MS (2008) Taguchi optimizaed synthesis of collagen-*g*-poly(acrylic acid)/kaolin composite superabsorbent hydrogel. Eur Polym J 44:1209–1216
11. Ren J, Kong W, Sun R (2014) Preparation of sugarcane bagasse/poly(acrylic acid-*co*-acrylamide) hydrogels and their application. BioResources 9:3290–3303
12. Wu Y, Zhou J, Ye C, Sun H, Zhao R (2010) Optimization synthesis of lignosulphonate-*g*-poly(acrylic acid-*co*-acrylamide) superabsorbent hydrogel based on the Taguchi method. Iran Polym J 19:511–520
13. Wang W, Wang A (2010) Synthesis and swelling properties of pH-sensitive semi-IPN superabsorbent hydrogels based on sodium alginate-*g*-poly(sodium acrylate) and polyvinylpyrrolidone. Carbohyd Polym 80:1028–1036
14. Işiklan N, Kurşun F, İnal M (2010) Graft copolymerization of itaconic acid onto sodium alginate using benzoyle peroxide. Carbohyd Polym 79:665–672
15. Saether HV, Holme HK, Maurstad G, SmidsrØd O, Stokke BT (2008) Polyelectrolyte complex formation using alginate and chitosan. Carbohyd Polym 74:813–821
16. Hua S, Wang A (2009) Synthesis, characterization and swelling behaviors of sodium alginate-*g*-poly(acrylic acid)/sodium humate superabsorbent. Carbohyd Polym 75:79–84
17. Yoo SH, Song YB, Chang PS, Lee HG (2006) Microencapsulation of α-tocopherol using sodium alginate and its controlled release properties. Int J Biol Macromol 38:25–30
18. Patel GM, Patel CP, Trivedi HC (1999) Ceric-induced grafting of methyl acrylate onto sodium salt of partially carboxymethylated sodium alginate. Eur Polym J 35:201–208
19. Tripathy T, Pandey SR, Karmakar NC, Bhagat RP, Singh RP (1999) Novel flocculating agent based on sodium alginate and acrylamide. Eur Polym J 35:2057–2072
20. Pourjavadi A, Zohuriaan-Mehr MJ (2002) Modification of carbohydrate polymers via grafting in air. 2. Ceric-initiated graft copolymerization of acrylonitrile onto natural and modified polysaccharides. Starch-Starke 54:482–488
21. Kalaleh HA, Tally M, Atassi Y (2013) Preparation of a clay based superabsorbent polymer composite of copolymer poly(acrylate-*co*-acrylamide) with bentonite via microwave radiation. Res Rev Polym 4:145–150
22. Yiğitoğlu M, Aydin G, Işiklan N (2014) Microwave-assisted synthesis of alginate-*g*-polyvinylpyrrolidone copolymer and its application in controlled drug release. Polym Bull 71:385–414
23. Rashidzadeh A, Olad A, Salari D, Reyhanitabar A (2014) On the preparation and swelling properties of hydrogel nanocomposite based on sodium alginate-*g*-poly(acrylic acid-*co*-acrylamide)/clinoptilolite and its application as slow release fertilizer. J Polym Res 21:344–359
24. Singh V, Tiwari A, Tripathi DN, Sanghi R (2004) Grafting of polyacrylonitrile onto guar gum under microwave irradiation. J Appl Polym Sci 92:1569–1575
25. Singh V, Tiwari A, Tripathi DN, Sanghi R (2006) Microwave enhanced synthesis of chitosan-*graft*-polyacrylamide. Polymers 47:254–260
26. Zhang J, Zhang S, Yuan K, Wang Y (2007) Graft copolymerization of *Artemisia* seed gum with acrylic acid under microwave and its water absorbency. J Macromol Sci A 44:881–885
27. Wan Z, Xiong Z, Ren H, Huang Y, Liu H, Xiong H, Wu Y, Han J (2011) Graft copolymerization of methyl methacrylate onto bamboo cellulose under microwave irradiation. Carbohyd Polym 83:264–269
28. Sen G, Singh RP, Pal S (2010) Microwave-initiated synthesis of polyacrylamide grafted sodium alginate: synthesis and characterization. J Appl Polym Sci 115:63–71
29. Işiklan N, Küçükbalcı G (2012) Microwave-induced synthesis of alginate-*graft*-poly(*N*-isopropylacrylamide) and drug release properties of dual pH- and temperature-responsive beads. E J Pharmacol Biopharm 82:316–331
30. Rani P, Mishra S, Sen G (2013) Microwave based synthesis of polymethyl methacrylate grafted sodium alginate: its application as flocculant. Carbohyd Polym 91:686–692
31. Tanan W, Saengsuwan S (2014) Microwave assisted synthesis of poly(acrylamide-*co*-2-hydroxyethyl methacrylate)/poly(vinyl alcohol) semi-IPN hydrogel. Energy Procedia 56:386–393
32. Montgomery DC (2001) Design and analysis of experiments. Wliey, New York
33. Pourjavadi A, Amini-Fazi MS, Ayyari M (2007) Optimization of synthetic conditions CMC-*g*-poly(acrylic acid)/Celite composite superabsorbent by Taguchi method and determination of its absorbency under load. Express Polym Lett 1:488–494
34. Pourjavadi A, Soleyman R, Bardajee Gh R, Seidi F (2010) γ-Irradiation synthesis of a smart hydrogel: optimization using

Taguchi method and investigation of its swelling behavior. Trans C: Chem Chem Eng 17:15–23
35. Zohuriaan-Mehr MJ, Kabiri K (2008) Superabsorbent polymers materials: a review. Iran Polym J 17:451–477
36. El-Sayed M, Sorour M, Abd El Moneem N, Talaat H, Shalaan H, El Marsafy S (2011) Synthesis and properties of natural polymers-grafted-acrylamide. World Appl Sci J 13:360–368
37. Ghasemzadeh H, Ghanaat F (2014) Antimicrobial alginate/PVA silver nanocomposite hydrogel, synthesis and characterization. J Polym Res 21:355–368
38. Ning PY (2011) Synthesis and characterisation of biodegradable superabsorbent polymer derived from sodium alginate. Masters thesis. Universiti Tunku Abdul Rahman, Kampar
39. Lanthong P, Kiatkamjornwong S (2006) Graft copolymerization, characterization, and degradation of cassava starch-*g*-acrylamide/itaconic acid superabsorbents. Carbodyd Polym 66:229–245
40. Gils PS, Ray D, Mohanta GP, Manavalan R, Sahoo PK (2009) Designing of new acrylic based macroporous superabsorbent polymer hydrogel and its suitability for drug delivery. Int J Pharm Pharm Sci 1:43–54
41. Hosseinzadeh H, Sadeghzadeh M, Badazadeh M (2011) Preparation and properties of carrageenan-*g*-poly(acrylic acid)/bentonite superabsorbent composite. J Boimater Nanobiotechol 2: 311–317
42. Schott H (1992) Swelling kinetics of polymers. J Macromol Sci B 31:1–9